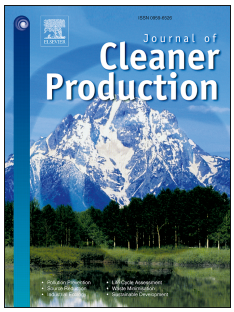

Ball-milled, solvent-free Sn-functionalisation of wood waste biochar for sugar conversion in food waste valorisation

Xiao Yang, Iris K.M. Yu, Daniel C.W. Tsang, Vitaliy L. Budarin, James H. Clark, Kevin C.-W. Wu, Alex C.K. Yip, Bin Gao, Su Shiung Lam, Yong Sik Ok

PII: S0959-6526(20)32347-7

DOI: https://doi.org/10.1016/j.jclepro.2020.122300

Reference: JCLP 122300

To appear in: *Journal of Cleaner Production*

Received Date: 1 December 2019

Revised Date: 10 April 2020

Accepted Date: 14 May 2020

Please cite this article as: Yang X, Yu IKM, Tsang DCW, Budarin VL, Clark JH, Wu KC-W, Yip ACK, Gao B, Lam SS, Ok YS, Ball-milled, solvent-free Sn-functionalisation of wood waste biochar for sugar conversion in food waste valorisation, *Journal of Cleaner Production* (2020), doi: https://doi.org/10.1016/j.jclepro.2020.122300.

CRediT author statement

CRediT (Contributor Roles Taxonomy) was introduced with the intention of recognizing individual author contributions, reducing authorship disputes and facilitating collaboration. The idea came about in 2015 at a Harvard workshop and it became a collaborative effort led by the Wellcome Trust and Digital Science, with input from publishers, including Elsevier, represented by Cell Press.

CRediT offers authors the opportunity to share an accurate and detailed description of their diverse contributions to the published work.

- The corresponding author is responsible for ensuring that the descriptions are accurate and agreed by all authors.
- The role(s) of all authors should be listed, using the relevant above categories.
- Authors may have contributed in multiple roles.
- CRediT in no way changes the journal's criteria to qualify for authorship.

CRediT statements should be provided during the submission process and will appear above the acknowledgement section of the published paper as shown further below.

Term	Definition
Conceptualization	Ideas; formulation or evolution of overarching research goals and aims
Methodology	Development or design of methodology; creation of models
Software	Programming, software development; designing computer programs; implementation of the computer code and supporting algorithms; testing of existing code components
Validation	Verification, whether as a part of the activity or separate, of the overall replication/ reproducibility of results/experiments and other research outputs
Formal analysis	Application of statistical, mathematical, computational, or other formal techniques to analyze or synthesize study data
Investigation	Conducting a research and investigation process, specifically performing the experiments, or data/evidence collection
Resources	Provision of study materials, reagents, materials, patients, laboratory samples, animals, instrumentation, computing resources, or other analysis tools
Data Curation	Management activities to annotate (produce metadata), scrub data and maintain research data (including software code, where it is necessary for interpreting the data itself) for initial use and later reuse
Writing - Original Draft	Preparation, creation and/or presentation of the published work, specifically writing the initial draft (including substantive translation)
Writing - Review & Editing	Preparation, creation and/or presentation of the published work by those from the original research group, specifically critical review, commentary or revision – including pre-or postpublication stages
Visualization	Preparation, creation and/or presentation of the published work, specifically visualization/ data presentation
Supervision	Oversight and leadership responsibility for the research activity planning and execution, including mentorship external to the core team
Project administration	Management and coordination responsibility for the research activity planning and execution
Funding acquisition	Acquisition of the financial support for the project leading to this publication

CRediT author statement

Xiao Yang: Conceptualization, Investigation, Data curation, Writing- Original draft preparation. **Iris K.M. Yu, Daniel C.W. Tsang:** Conceptualization, Methodology, Investigation, Writing- Reviewing and Editing, Project administration, Funding acquisition. **Vitaliy L. Budarin, James H. Clark, Kevin C.-W. Wu, Alex C.K. Yip, Bin Gao, Su Shiung Lam, Yong Sik Ok**: Writing- Reviewing and Editing, Validation, Visualization, Supervision.

Ball-milled, solvent-free Sn-functionalisation of wood waste biochar for sugar conversion in food waste valorisation

Xiao Yang[a,b], Iris K.M. Yu[a,c], Daniel C.W. Tsang[a,*], Vitaliy L. Budarin[c], James H. Clark[c], Kevin C.-W. Wu[d], Alex C.K. Yip[e], Bin Gao[f], Su Shiung Lam[g], Yong Sik Ok[b,#]

[a] *Department of Civil and Environmental Engineering, The Hong Kong Polytechnic University, Hung Hom, Kowloon, Hong Kong, China*

[b] *Korea Biochar Research Center, Division of Environmental Science and Ecological Engineering, Korea University, Seoul 02841, Republic of Korea*

[c] *Green Chemistry Centre of Excellence, Department of Chemistry, University of York, York, YO10 5DD, United Kingdom*

[d] *Department of Chemical Engineering, National Taiwan University, Taipei 10617, Taiwan*

[e] *Energy and Environmental Catalysis Group, Department of Chemical and Process Engineering, University of Canterbury, Christchurch 8041, New Zealand*

[f] *Department of Agricultural and Biological Engineering, University of Florida, Gainesville, Florida 32611, United States*

[g] *Pyrolysis Technology Research Group, Eastern Corridor Renewable Energy Group, School of Ocean Engineering, Universiti Malaysia Terengganu, 21030 Kuala Nerus, Terengganu, Malaysia*

[*]Corresponding author: *dan.tsang@polyu.edu.hk (D.C.W. Tsang),*

[#]Co-corresponding author: *yongsikok@korea.ac.kr (Y.S. Ok)*.

Abstract

The use of biomass wastes for biochar production is a promising waste management option, and biochars can be potentially applied in the food waste recycling industry to produce value-added chemicals. In this study, an advanced Sn-functionalised biochar catalyst was synthesised via a novel solvent-free ball milling protocol to facilitate the isomerisation of glucose to fructose. Raw wood biomass (W) and its derived biochars pyrolysed at low (LB, 400 °C) and high (HB, 750 °C) temperatures were investigated as catalyst supports. The interactions between Sn and the carbonaceous supports were related to the surface chemistry of the catalysts. The raw W had a functional group-enriched surface, which provided more active sites for anchoring Sn, resulting in higher metal loading on the support compared to LB and HB. The annealing temperature was another critical factor determining the amount and speciation of loaded Sn. Catalytic conversion experiments indicated that SnW annealed at 750 °C exhibited the best fructose yield (12.8 mol%) and selectivity (20.2 mol%) at 160 °C for 20 min. The catalytic activity was mainly determined by the quantity and nature of active Sn sites. This study elucidated the roles of the carbon support and its surface chemistry for synthesising biochar-supported catalysts, highlighting a simple and green approach for designing effective solid catalysts for sustainable biorefineries.

Keywords: solvent-free synthesis; heterogeneous catalysis; engineered biochar; metal-carbon interactions; sustainable waste management.

1. Introduction

The increase in biomass waste generation (e.g., forestry/agricultural and food wastes) has posed a critical environmental challenge calling for a sustainable solution. As suggested by various laboratory and pilot tests, the conversion of biomass into biochars is a promising waste management option, which is potentially superior to conventional treatments, such as landfill disposal and open burning with low energy transformation efficiency that burdens the environment (Ok et al., 2015). Biochar production costs only 3-6% of the commercial activated carbon (Jung et al., 2019), and it has the benefits of tuneable properties and easy manufacture, which are advantageous for carbonaceous material engineering and green chemistry. Besides environmental remediation (Cho et al., 2019; Ruan et al., 2019) and novel material synthesis (Wang et al., 2019), emerging applications of engineered biochars recently have been explored in green biorefineries (Xiong et al., 2017).

Glucose is a six-carbon sugar that can be derived from biomass—e.g., starch-rich bread and rice wastes (Yu et al., 2018; Cao et al., 2018). It undergoes isomerisation to form fructose that can be further converted into a wide variety of platform chemicals and energy derivatives, which reduce the dependence on fossil fuels and mitigate carbon emissions (Zhu et al., 2016a; Xiong et al., 2019; Chen et al., 2017). Glucose isomerisation can be catalysed by Lewis acids (e.g., Sn^{4+}, Al^{3+}) or Brønsted bases (i.e., OH^-). Lewis acids facilitate the ring-opening of glucose and promote isomerisation via an intramolecular C2-C1 hydride shift (Hu et al., 2017; Caratzoulas et al., 2014), while Brønsted bases catalyse an O2-O1 hydrogen

transfer (Chen et al., 2018).

Solid Lewis acid catalysts can be synthesised via the impregnation of metals on graphite/graphene oxide and carbon nanotubes (Xiao et al., 2017; Yu et al., 2019b). Biochars emerge as an attractive alternative supporting material in view of the low production cost and favourable eco-friendliness (Yu et al., 2019a; Yang et al., 2019a). Previous research has focused on the physicochemical properties of carbon-based catalysts (e.g., porosity, morphology, acid-base properties) (Qin et al., 2019; Wan et al., 2019), yet seldom explored the interactions between carbon support and adsorbed species that could determine the Lewis acidity of catalysts. It has been proposed that metal-support interactions can take place via charge transfer, surface complexation, and other mechanisms (Qiang et al., 2007; Sun et al., 2019), which may facilitate high loading rates and homogeneous distribution of active sites (Zhukovskii et al., 2000). The binding of metals to biochar can be improved by enriching its structural surface defects (e.g., terraces, steps, and kinks) (Lobos et al., 2016). However, it is uncertain how metal speciation and surface chemistry vary with the metal-biochar interaction, and whether adverse effects (e.g., inactive species formation) can be avoided. In this study, we prepared Sn-impregnated biochars that provide a good opportunity to investigate the relationship between catalytic activity and metal-support interactions. Sn has been suggested to be an outstanding Lewis acid catalyst in heterogeneous and homogeneous systems in biorefinery studies (Bermejo-Deval et al., 2014; Yu et al., 2018).

In conventional catalyst synthesis, the use of solvents is often indispensable to facilitate

dispersion and mixing for better contact between the loading materials and support (Rightmire et al., 2016). As for greener protocols, mechanochemical technology, such as ball milling, is based on the direct mixing of materials under solvent-free conditions, which allows for simple and safe operation with potential industrial applicability (James et al., 2011; Takacs, 2018). The shear forces and powerful extrusion in ball milling can activate the catalyst support surface by reducing the particle size and creating new defects, which would alter the surface chemistry—e.g., functionality, hydrophobicity, and polarity (Zhang et al., 2019). Ball milling has been applied to modify graphene, carbon nanotubes, and metal–organic frameworks (Kathryn et al., 2013; Franco et al., 2017; Ouyang et al., 2016; Lin et al., 2017), while its utilisation for functionalising the biochars is still in its infancy and deserves investigation to develop sustainable biochar-based catalysts.

This study aims to synthesise a series of Sn-functionalised biochars (SnBCs) as Lewis acid-type heterogeneous catalysts using ball milling. Their catalytic activity was evaluated for the isomerisation of glucose to fructose in water under microwave heating, an important reaction in biomass waste upcycling for the synthesis of value-added chemicals. Three different carbon-based supports were studied: wood biomass (W, not pyrolysed) and low- and high-temperature wood biochar (LB and HB, respectively), which were pyrolysed at 400 and 750 °C, respectively. The role of the physicochemical properties of the carbonaceous supports and effect of metal-support interactions induced by different annealing temperatures on the fructose yield and selectivity were studied. The environmental sustainability of the proposed

100 SnBC catalyst was evaluated by recycling and metal leaching tests.

101

102 **2. Materials and Methods**

103 *2.1.Materials*

104 Wood waste is a significant waste stream and prospective feedstock in biorefineries
105 (Hassan et al., 2019). Mixed wood waste in the form of sawdust (< 2 mm), which was
106 collected from the Industrial Centre at the Hong Kong Polytechnic University, was used as
107 the carbon precursor, in view of its good performance in our recent studies of biochar-based
108 catalysts (Yang et al., 2019a; Yu et al., 2019a). The wood biomass was air-dried at 60 °C
109 overnight until its weight appeared to be constant. $SnCl_4 \cdot 5H_2O$ (98%, Sigma-Aldrich) was
110 used as the Sn source. For sample preparation, catalysis reactions, and calibration of the
111 analyser, the chemicals of analytical grade were used as received.

112 Wood biomass and its two derived biochars were used as bio-based support for the
113 synthesis of SnBCs. Biochars were produced via slow pyrolysis under nitrogen purging (150
114 mL min^{-1}). Wood biomass was subjected to pyrolysis at 400 and 700 °C for 2 h in a Carbolite
115 tubular furnace to obtain LB and HB, respectively. The prepared support was composited
116 with $SnCl_4 \cdot 5H_2O$ at a weight ratio of 10:1 using a planetary ball mill (DECO-PBM-AD-
117 0.4L). Approximately 5 g of material was added to a 100 mL Teflon jar that contained 100 g
118 of balls and was operated at 900 rpm for 2 h in air. The rotation direction was changed every
119 10 min. The energy consumption for ball milling was estimated as 0.5 kWh, considering the

instrument power of 0.25 kW and a milling time of 2 h. The resultant samples were then annealed at 500, 750, or 900 °C under N_2 and were labelled as SnXY, where X is the support, and Y is the catalyst annealing temperature. All solid catalysts were stored in vials for subsequent experiments.

2.2.Characterisation of SnBC catalysts

Thermochemical changes were monitored in the range of room temperature to 1000 °C at a heating rate of 10 °C min^{-1} in Ar atmosphere using a Thermo plus EVO2 (Rigaku) thermogravimetric analysis (TGA) instrument. The morphology, structure, and surface composition of the samples were analysed using a VEGA3 XM (TESCAN) field-emission scanning electron microscopy (SEM) apparatus equipped with an energy dispersive spectroscopy (EDS) system. The crystalline textural features were recorded using a SmartLab (Rigaku) X-ray diffraction (XRD) device using Cu Kα radiation (1.5460 Å). The porosity parameters were evaluated using N_2 adsorption–desorption isotherms, which were collected utilizing an ASAP 2020 (Micromeritics) surface area and porosity analyser. Micro-Raman spectroscopy (Renishaw) was carried out using a light source with an excitation wavelength of 532 nm. The ratios of the intensities of the D and G peaks (1350 and 1590 cm^{-1}) (I_D/I_G) of all samples were calculated using their Raman spectra (Igalavithana et al., 2018).

Surface chemistry and metal speciation were evaluated using a Frontier (PerkinElmer) Fourier transform infrared (FTIR) spectroscopy instrument and a K-Alpha (Thermo Fisher Scientific) X-ray photoelectron spectroscopy (XPS) device. The FTIR and XPS spectra were

manipulated using the OMNIC and XPSpeak41 software programmes, respectively.

The total amount of Sn loaded onto each catalyst was determined using an FMX36 SPECTROBLUE inductively coupled plasma mass spectrometer after the samples were completely digested using aqua regia, according to the modified United States Environmental Protection Agency Method 3051A.

2.3.Glucose isomerisation to fructose over SnBC catalysts

The glucose isomerisation process was conducted in batches following the protocol previously described in the literature (Yang et al., 2019a). In brief, 0.5 g of glucose, 0.25 g of SnBCs, and 10 mL of deionised water were added to a 100 mL vessel and were stirred until a homogeneous mixture was obtained. The vessel was sealed and heated at 160 °C for 20 min in an ETHOS UP (Milestone) microwave reactor in air (ramp time of 5 min). The catalyst dosage and catalytic test settings were mainly based on the preliminary experiment and were intended to achieve discernible differences in catalytic activity and selectivity between different synthesised catalysts, which may not be optimal. Future efforts should be made in that direction. The liquid products were collected, filtered, and diluted with deionised water by a factor of four before being subjected to high-performance liquid chromatography (HPLC) analysis. The details for analytical conditions and calculation of product yield and selectivity are shown in SI.

3. Results and Discussion

3.1.Characteristics of biochar-supported Sn catalysts prepared via ball milling

The synthesis of the SnBC catalysts consisted of two steps: (1) the uniform dispersion of the Sn source onto the supporting materials (HB, LB, and W) using ball milling; and (2) the activation of the Sn-support mixture at different annealing temperatures. Each Sn-support composite without annealing was subjected to TG-DTA to investigate its heat-induced transformation (Fig. 1). The significant decrease in mass (7.13%) of the SnHB sample at 100–200 °C could be attributed to the volatilisation of the surface-free $SnCl_4$ (Freiser, 1959), which was absent from the TGA patterns of SnLB and SnW. This suggests the weak interaction between Sn and HB after ball milling. As illustrated in Table 1, the O/C ratios of both LB and W were higher than that of HB because the latter lost more O-containing functional species during the high-temperature treatment (Yang et al., 2018). The surface O-containing groups could act as active sites for anchoring Sn. At 230–500 °C, the SnW and SnLB samples exhibited a major mass decay of 53.5% and 11.5%, respectively. Significant mass loss (~75%) in this temperature range was also noted in the TGA pattern of the raw W (Yu et al., 2019a). This could be attributed to the thermal decomposition of the lignocellulosic fraction of W and degradable carbon moieties remaining in the partially pyrolysed LB (Igalavithana et al., 2017). At temperatures above 500 °C, the mass changes of all samples became minor considering the plateaus in the DTG curves (Fig. 1b).

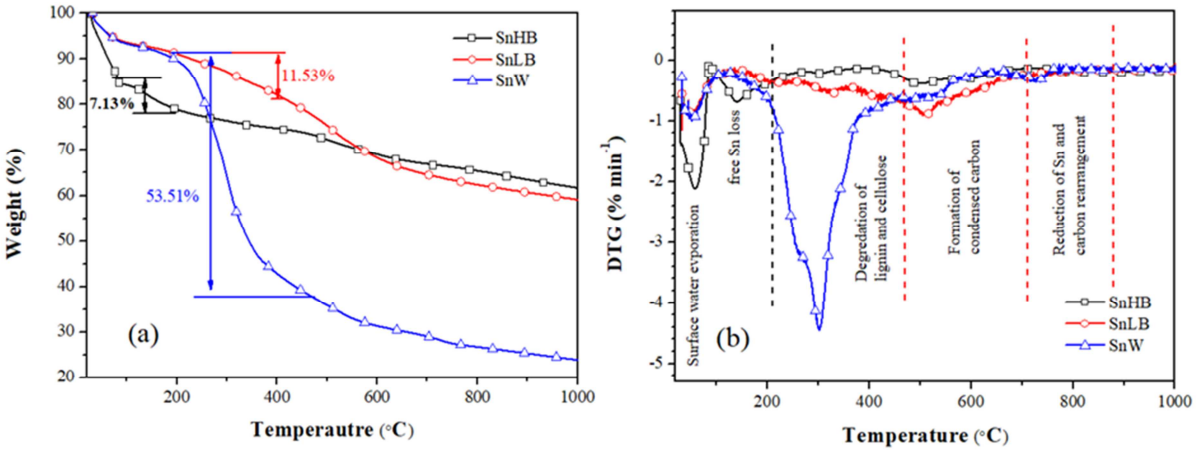

178

179 **Figure 1.** (a) Thermogravimetric analysis and (b) differential thermogravimetric analysis
180 curves of SnW, SnLB, and SnHB obtained after milling different supporting materials with
181 $SnCl_4 \cdot 5H_2O$ (without annealing).

182 In general, the FTIR spectra of W and LB and their derivative samples presented stronger
183 absorption at 1000-1750 cm^{-1} than those of HB and its derivatives (Fig. 2a-c). This is in a
184 good agreement with the higher O/C ratios for W and LB that implied more abundant
185 functional groups on their surfaces (Table 1). Ball milling with Sn (without annealing)
186 resulted in an increased broad band at 3400 cm^{-1} that represents the O-H stretching, possibly
187 due to the formation of new surface defects in oxygen-containing atmosphere (Li et al.,
188 2020). The largely preserved O functionalities and new defects on the supporting materials
189 may enhance the interaction with Sn via surface complexation. The XRD patterns of the raw
190 and ball-milled samples were similar and displayed amorphous characteristics (Figs. 2d–f),
191 suggesting that ball milling may not provide sufficient energy for converting the Sn precursor
192 ($SnCl_4$) to crystalline minerals. After annealing at 500 ^oC, SnO_2 could be observed, and it
193 further transformed to metallic Sn at the high temperatures of 750 and 900 ^oC. The formation
194 of metallic Sn (2θ = 30.64°, 32.02°, and 44.91°) was more significant in the SnW750 and

195 SnW900 samples than in the annealed SnLB and SnHB samples, suggesting the stronger
196 carbothermal reduction capacity of W that could release more reducing gases (H_2, CO) during
197 thermal treatment (Sikarwar et al., 2016).

198 **Table 1.** Physicochemical characteristics of supporting materials and synthesised samples.

	BET surface area	t-plot micropore surface area	t-plot external surface area	Pore volume	Average pore diameter	O/C	I_D/I_G
	$m^2\ g^{-1}$			$cm^3\ kg^{-1}$	nm		
HB	179.8	123.9	55.9	49.6	4.54	0.04	0.56
LB	85.4	53.7	31.8	35.4	6.45	0.15	0.82
W	0.73	0.02	0.71	7.64	38.0	0.71	-
SnHB	3.07	0.01	3.06	99.9	53.1	0.09	0.58
SnHB500	65.6	31.9	33.7	40.6	9.81	0.08	0.79
SnHB750	382.7	311.7	71.0	73.5	6.33	0.07	0.82
SnHB900	137.9	59.5	78.5	114.4	5.40	0.07	0.96
SnLB	2.86	0.01	2.85	34.1	45.6	0.20	0.84
SnLB500	44.7	7.99	36.7	58.2	11.8	0.09	0.79
SnLB750	125.2	73.2	52.0	103.0	8.29	0.07	0.82
SnLB900	110.9	53.4	57.5	89.0	8.74	0.04	0.97
SnW	0.33	0.01	0.32	8.10	43.8	0.54	-
SnW500	50.6	11.6	39.0	16.6	5.21	0.13	0.63
SnW750	131.0	72.6	58.4	85.0	5.58	0.08	0.81
SnW900	138.2	79.9	58.3	79.6	5.32	0.13	0.91

199 BET - Brunauer–Emmet–Teller; O/C - oxygen/carbon ratio; I_D/I_G - ratio of the intensities of the D and G Raman peaks; W - wood biomass, LB
200 and HB - biochars pyrolysed at low (400 °C) and high (750 °C) temperature, respectively; SnW, SnLB, and SnHB - Sn-functionalised samples;
201 500, 750, and 900 are the annealing temperatures.
202
203

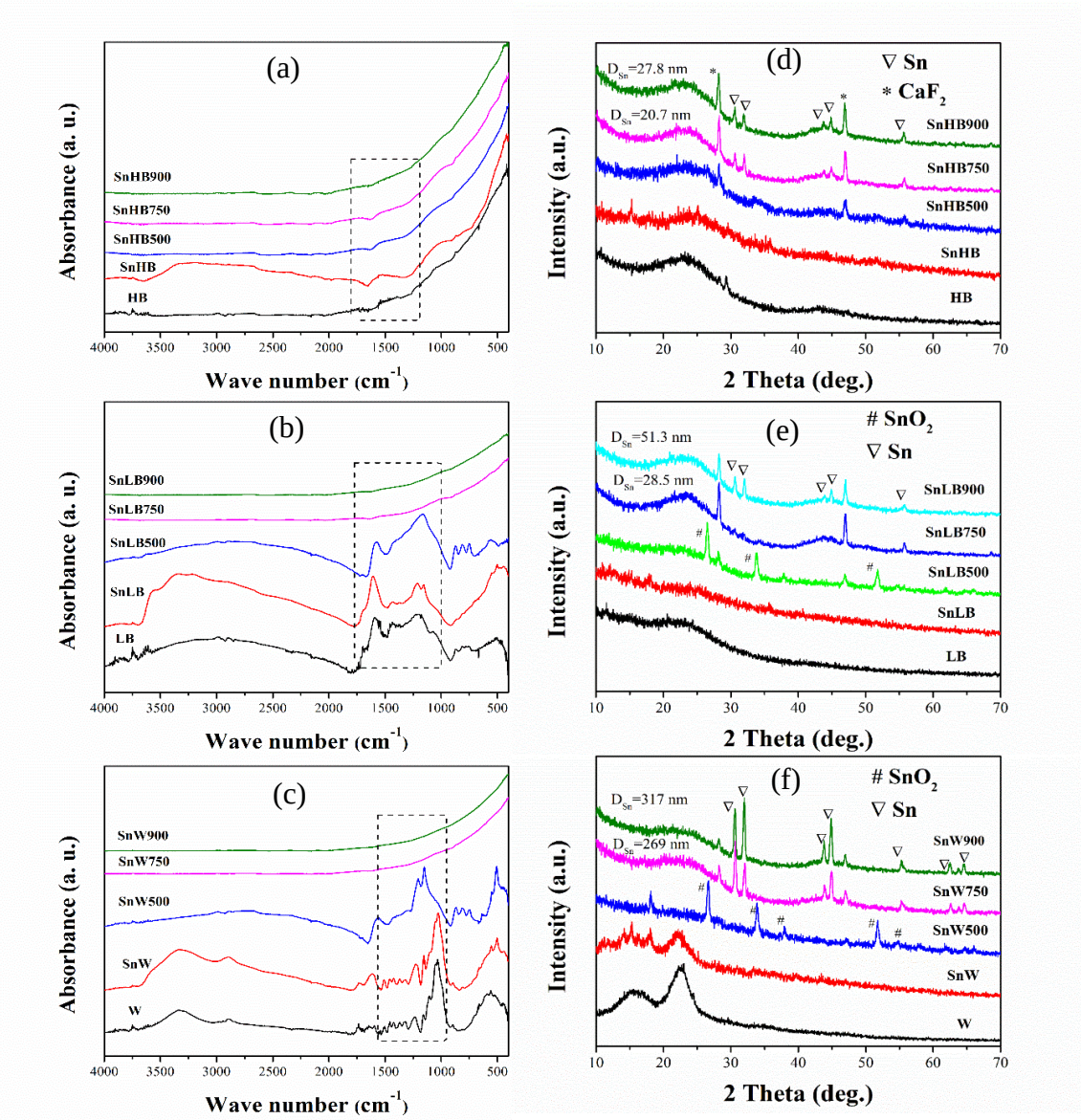

Figure 2. (a–c) Fourier transform infrared spectra and (d–f) X-ray diffraction patterns of synthesised samples, where W is wood biomass; LB and HB are biochars pyrolysed at low (400 °C) and high (750 °C) temperature, respectively; SnW, SnLB, and SnHB are Sn-functionalised samples; and 500, 750, and 900 °C are the annealing temperatures.

The SEM-EDS images reaffirmed the incorporation of Sn species in the W, LB, and HB supporting materials after ball milling and annealing (Fig. 3). The proportion of Sn followed the same order for the quantity of O-containing functionalities – W > LB > HB (Table 1). Surface Sn content of approximately 10 wt% was observed in SnW, which was equivalent to the initial Sn dosage. However, the SnLB and SnHB presented much lower surface Sn contents than the Sn loading amount: 2.64 and 1.24 wt%, respectively. Carbon supports (W)

featuring larger amount of sp^3 carbons (high I_D/I_G ratio) and more hydrophilic surface (high O/C ratio) can present higher affinity for Sn precursor, leading to higher possibility of forming Sn complexes during the ball milling process (Table 1).

After annealing at 500 °C, the Sn dot contour profiles of all samples were analogous to the catalyst shape (Fig. 3). However, further increasing the annealing temperature led to a decrease in Sn dot intensity and different Sn distribution patterns. In particular, the clusters of Sn dots can be observed in SnW750/900. Calculations using the XRD results and Scherrer equation confirmed that nanosized metallic Sn particles were formed in SnHB750 (20.7 nm) and SnLB750 (28.5 nm), whereas microsized metallic Sn particles were observed in SnW750 (269 nm). The higher surface Sn concentration in SnW possibly induced metal agglomeration to larger particles during the annealing process, which became more severe as the annealing temperature increased (Fig. 3). Hence, selecting the appropriate starting materials is critical for the preparation of carbon-based catalysts via the ball milling process, because their properties (particularly for surface functional groups and carbonisation degree) play a key role in determining the extent of metal loading, speciation, morphology, and distribution.

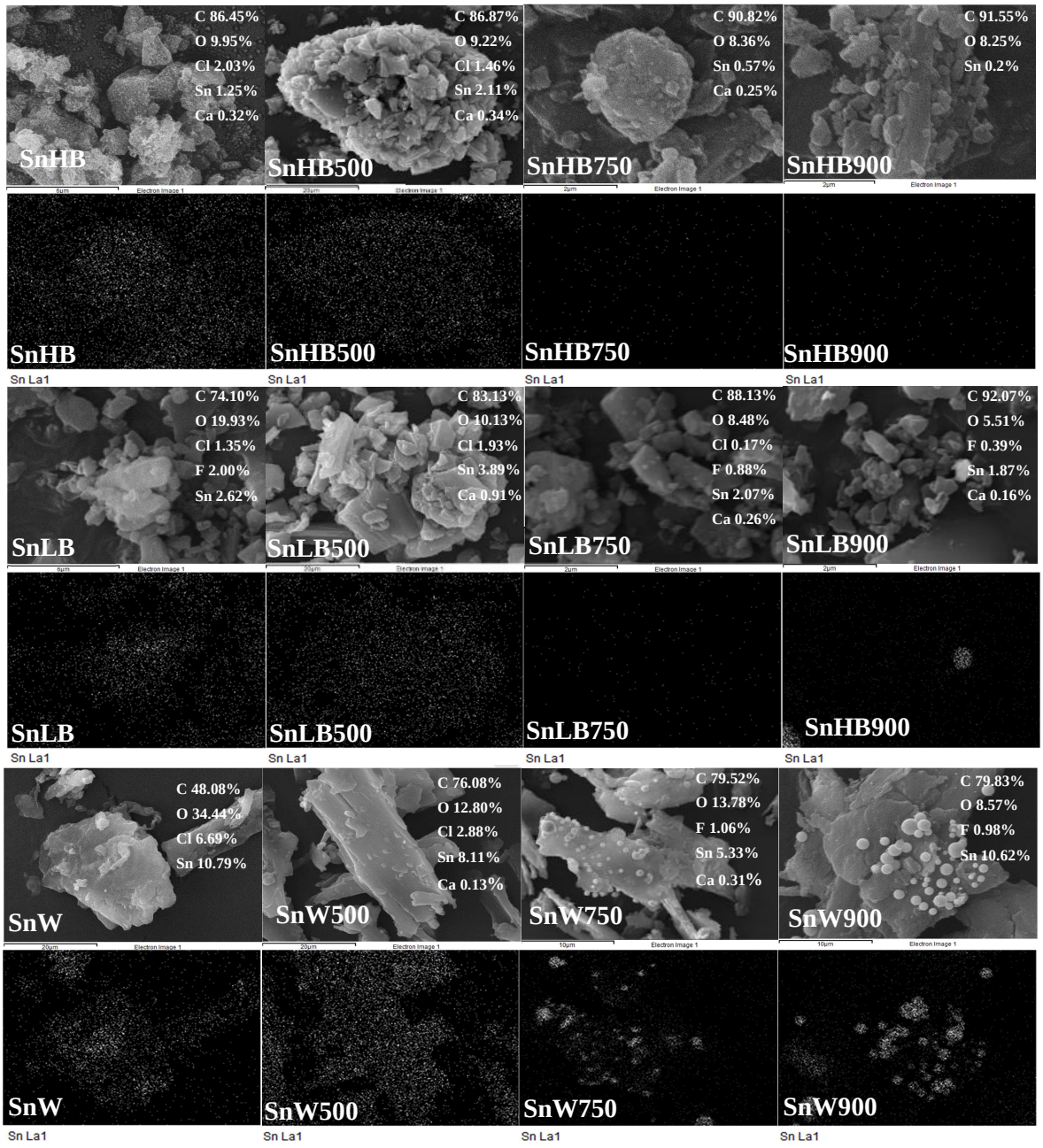

Figure 3. Scanning electron microscopy images and energy dispersive X-ray spectroscopy Sn mapping results of synthesised samples, where SnW, SnLB, and SnHB are Sn-functionalised wood biomass (W) and biochars pyrolysed at low (400 °C) and high (750 °C) temperatures, respectively (LB and HB respectively); 500, 750, and 900 °C are the annealing temperatures.

It was noted that when Sn salt was milled with the supports, the surface area and average pore size significantly decreased (Table 1), possibly due to pore blocking by the introduced Sn (Baca et al., 2008). However, the porosity of all ball-milled samples could be developed after annealing, as a result of new pore formation and partial volatilisation of carbon moieties

and surface-adsorbed Sn. This effect was more noticeable when the annealing temperature increased from 500 to 750 °C, whereas the samples annealed at 900 °C displayed only small increases or even a decrease in porosity. The I_D/I_G ratios of all samples increased as the annealing temperature increased, implying that more defects were formed and possibly facilitated catalytic conversion. However, the O/C ratio, which is also an index for surface hydrophobicity (Yang et al., 2019b), showed little dependence on the annealing temperature (Table 1).

3.2.Important role of initial support materials for catalytic conversion

When the SnBC samples annealed at 500 °C were used as catalysts (160 °C, 20 min; Fig. 4), the fructose yield was negligible regardless of the support materials and despite their higher amounts of total Sn (e.g., > 100 mg g^{-1} Sn for SnW500) compared to those annealed at 750 and 900 °C. This indicated that the catalytic activity strongly depended on the availability of active Sn sites rather than the total surface Sn content. At a low annealing temperature, some thermal-sensitive volatiles, such as CO_2 and Cl_2, would be generated via decomposition (Sikarwar et al., 2016), reacting with the loaded Sn to form chemically inert SnO_2, which is inactive towards the glucose isomerisation (Yu et al., 2018). Previous studies reported that the tetra-coordinated Sn^{4+} sites would be the major contributors for catalysing glucose isomerisation, rather than the octahedral-coordinated Sn^{4+}, such as SnO_2, which exhibited poor Lewis acidity (Dijkmans et al., 2015).

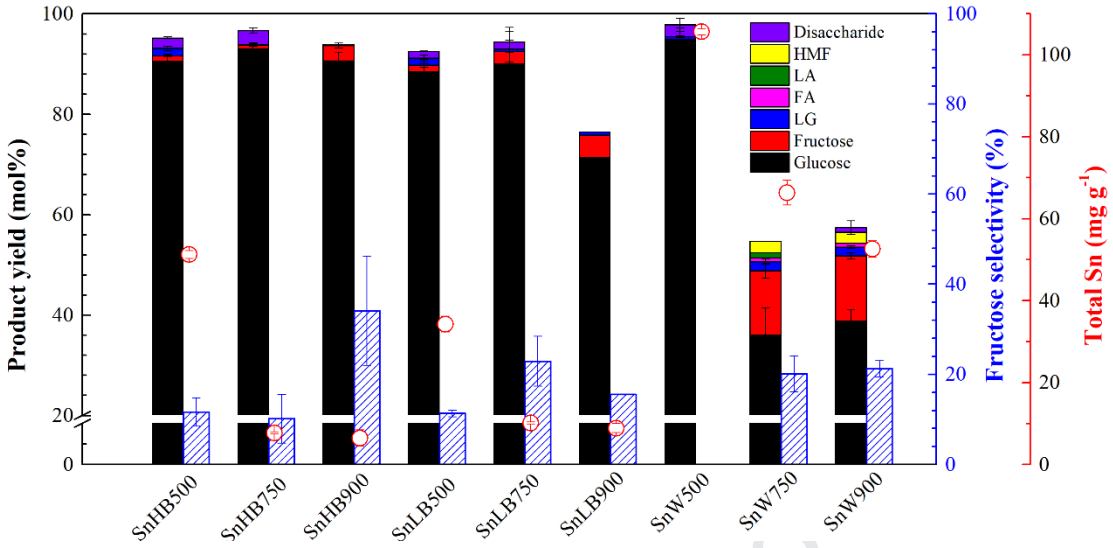

Figure 4. Fructose yield and selectivity obtained from microwave-assisted glucose isomerisation tests over different synthesised catalysts (conversion conditions: 160 ºC for 20 min in water), where HMF, LA, FA, and LG are 5-hydroxymethylfurfural, levulinic acid, formic acid, and levoglucosan, respectively; SnW, SnLB, and SnHB are Sn-functionalised wood biomass (W) and biochars (LB and HB) pyrolysed at low (400 °C) and high (750 °C) temperatures, respectively; and 500, 750, and 900 °C are the annealing temperatures.

For the samples produced using HB, SnHB900 achieved a higher fructose yield and selectivity than SnHB750 (Fig. 4), despite the lower BET surface area of the former (Table 1). The XRD patterns indicated that a metallic Sn phase was formed after annealing at 750 °C or above (Figs. 2d–f), revealing the occurrence of a redox reaction at the interface region via electron transfer between the adsorbed metal and carbon support. This carbothermal reduction could activate the inactive Sn species (SnO_2) during high-temperature annealing. The presence of Sn-Sn^{4+}@C was probably relevant for the superior catalytic activity (Section 3.3). It is noteworthy that the catalytic activity of the Sn-functionalised biochar catalysts was affected by the choice of initial supporting materials, i.e., SnW750 and SnW900 were the most active (Fig. 4). The metal-support interactions could be the decisive factor for

283 controlling the catalytic activity of the Sn-functionalised biochar catalysts prepared by ball
284 milling.
285
286 *3.3.Effect of annealing temperature on catalytic conversion*
287 Fig. 4 indicates that the annealing temperature was an important parameter, and heating at
288 750 or 900 °C was essential for the formation of active Sn on the ball-milled biochar
289 catalysts. To elucidate the valence states of the Sn dopants in the biochar catalysts, the XPS
290 spectra in the vicinity of Sn 3d were deconvoluted into three subpeaks (Figs. 5a–c),
291 corresponding to Sn^{4+}, Sn^{2+}, and Sn^{0} (Zhu et al., 2016b). The results indicated that the
292 binding energies of the two characteristic peaks of Sn 3d (Sn $3d_{5/2}$ and Sn $3d_{3/2}$) of SnW750
293 and SnW900 shifted towards the higher energy region compared to the reference values. This
294 shift often is associated with the occurrence of strong metal-support interactions and partial
295 reduction of SnO_2 to metallic Sn (Ma et al., 2011). Therefore, increasing the annealing
296 temperature could promote the electron-donor effect between the metal and carbon support,
297 thereby enriching the d-electron density of Sn 3d (Pino et al., 2014).
298

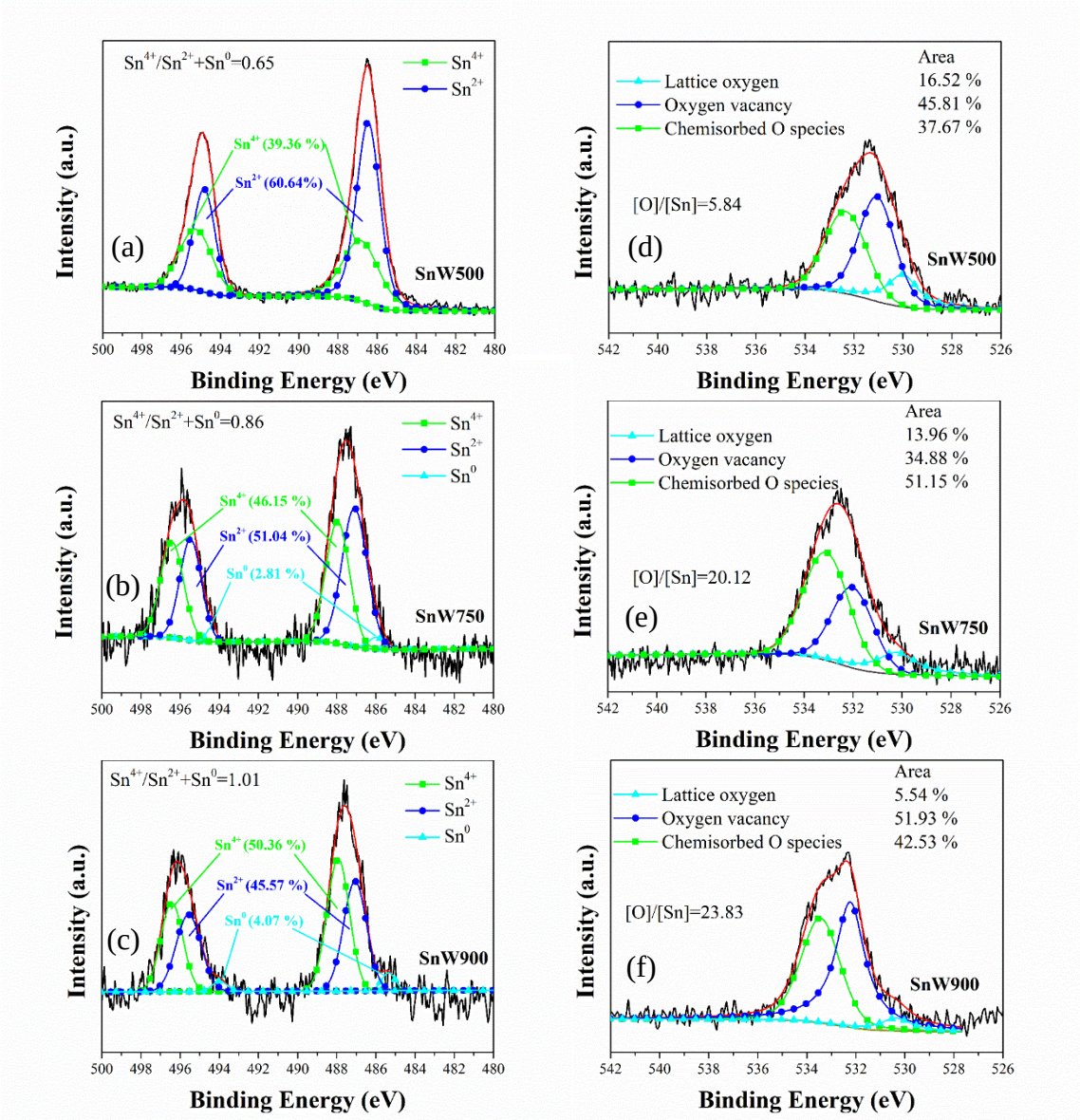

Figure 5. X-ray photoelectron spectroscopy (XPS) (a–c) Sn 3d and (d–f) O 1s spectra of Sn-functionalised biochar catalysts (SnW500, SnW750, and SnW900) prepared at three representative temperatures (500, 750, and 900 °C, respectively) using wood biomass (W) as supporting material. Ratios were calculated from the XPS results using their atomic numbers.

At the lowest annealing temperature, the Sn species in SnW500 mainly consisted of tin oxides—i.e., SnO_2 and SnO—and were chemically inert and exhibited little catalytic capacity despite the large amount of Sn. The ratio of $[Sn^{4+}]/([Sn^{2+}]+[Sn^{0}])$ increased from 0.65 to 1.01 as the annealing temperature increased from 500 to 900 ^{o}C. It appears that the interconversion of the multiple valence states of Sn species (Zhong et al., 2014) could induce the formation of

active tetra-coordinated Sn^{4+} (Fig. 6), possibly accounting for the superior catalytic performance of SnW900 (Fig. 4). In addition, the annealing process would facilitate the substitution of the metal in the carbon matrices, thereby inducing distortion and defects in the biochar catalysts owing to the larger ionic radius of Sn^{4+} compared to that of C. This could be reflected by the increasing I_D/I_G ratio as the annealing temperature increased (Table 1), which may also contribute to the increased catalytic activity.

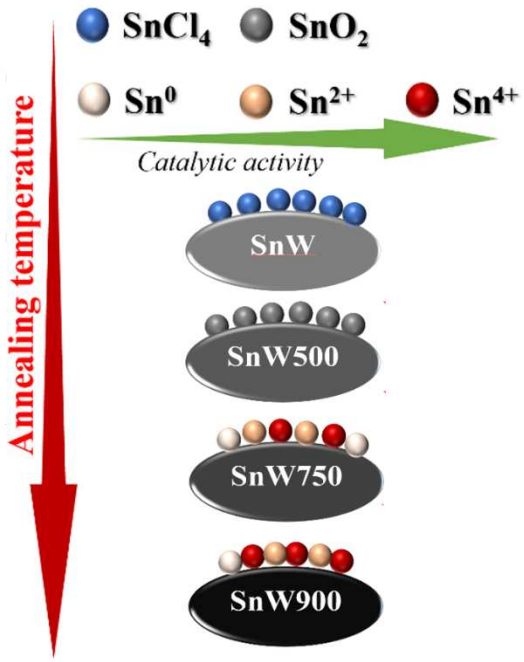

Figure 6. Schematic diagram for the transformation of Sn-biochar catalysts.

The O 1s XPS signals were deconvoluted into three peaks at 530.2, 531.3, and 533.1 eV (Figs. 5d–f), which were ascribed to three types of O species: lattice O, O vacancies, and chemisorbed O species, respectively (Jung et al., 2012). The content of lattice O decreased from 16.5 to 5.5% as the annealing temperature increased from 500 to 900 ^{o}C. This could be caused by the replacement of carbon atom with a lower valence metal (e.g., Sn^{2+}) leading to charge compensation in the catalysts. The surface [O]/[Sn] ratio of SnW500 was 5.84, which was lower than those for SnW750 (20.1) and SnW900 (23.8), suggesting that the Sn

speciation varied with annealing temperatures (Farahani et al., 2014). While the XPS valance band pattern of SnW500 exhibited four sub-bands at 0-20 eV (Fig. 7), they disappeared from the spectra of SnW750 and SnW900 with a new C 2s peak emerging (Zatsepin et al., 2016). The BET surface areas of SnW750 and SnW900 were 159% and 173% higher than that of SnW500, which may be partly ascribed to the surface etching of the carbon support in the presence of Sn (Yu et al., 2019c). The annealing temperature not only affected the transformation of active Sn species but also influenced the surface chemistry and structure of the biochar catalysts, and thereby their catalytic performance.

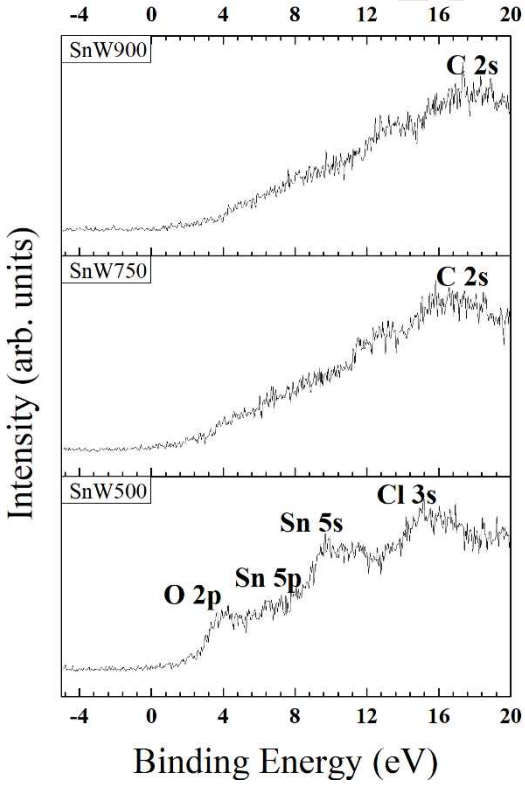

Figure 7. X-ray photoelectron spectroscopy valence band spectra of Sn-functionalised wood biomass (W)-based catalysts annealed at 500, 750, and 900 °C: SnW500, SnW750, and SnW900, respectively.

3.4.Evaluation of recyclability of SnBC catalysts prepared by ball milling

The adsorption tendency by the SnBC catalysts was investigated. The SnBC catalysts adsorbed only a trivial amount of sugars (Table 2), which was favourable for the rapid separation of catalysts after conversion, similar to the commonly used heterogeneous acid catalysts, such as Amberlyst-15 and sulfonated biochar (Hafizi et al., 2016; Cao et al., 2018).

Table 2. Adsorption properties of ball-milled Sn-biochar catalysts towards glucose and fructose (initial concentration was 0.5 g/10 mL, and equilibrium was reached in 30 min at room temperature).

Catalyst	Adsorbed capacity of chemicals per gram of catalyst (mg g^{-1})	
	Glucose	Fructose
SnHB500	1.35	1.12
SnHB750	1.72	2.01
SnHB900	0.17	0.44
SnLB500	1.83	1.72
SnLB750	0.89	1.23
SnLB900	0.85	1.34
SnW500	0.08	0.14
SnW750	1.47	1.84
SnW900	1.05	1.28

For the reusability test, the SnBC catalysts were separated and recovered by filtration after each reaction cycle. The liquid fraction was used to analyse the product distribution, and the solid fraction was sonicated with deionised water four times before the subsequent re-use. During the first recycling experiment, the fructose yield decreased from ~13 to 4 mol% for SnW750 and SnW900, which remained nearly constant in the second and third runs (Fig. 8). The XRD results (Fig. S1) indicated that SnO_2 emerged after the reaction; in accordance, the XPS spectra (Fig. S2) showed an increased Sn^{4+} content of 77% for the RSnW750. In addition, the leaching test (Fig. S3) showed ~20% Sn leaching in the first cycle for both SnW750 and SnW900 catalysts, which was consistent with the SEM-EDS mapping showing a decreased surface Sn content (Fig. S4). The total Sn content remained almost constant in

the next three cycles (Fig. S3). Therefore, the reduced catalytic performance may be associated with the transformation of active Sn species to inactive species and with Sn leaching. The chemical transformation of the SnBC catalysts deserves future studies to improve the recycling performance under hydrothermal conditions. From a long-term perspective, the advantages of the ball milling process for biochar-supported catalyst synthesis should be demonstrated via life cycle analysis and techno-economic assessment. Fair comparison can be carried out when energy use in ball milling and solvent use in conventional protocols are evaluated using the same metrics, e.g., environmental impacts and costs.

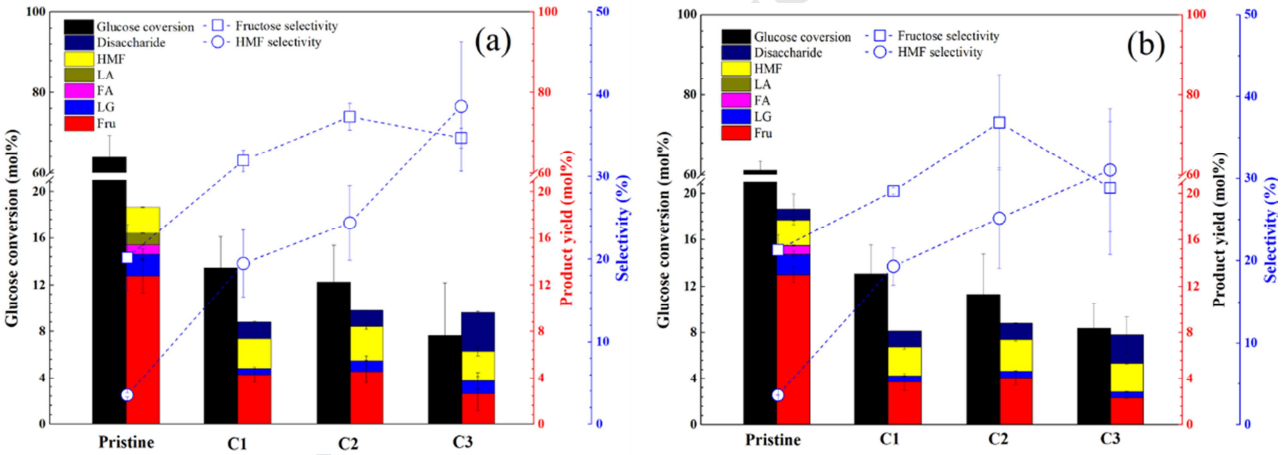

Figure 8. Reusability tests of (a) SnW750 and (b) SnW900 for glucose isomerisation to fructose (three reaction cycles: C1–C3 were conducted under the same catalytic conditions at 160 °C for 20 min), where HMF, LA, FA, Fru, and LG are 5-hydroxymethylfurfural, levulinic acid, formic acid, fructose and levoglucosan, respectively; and SnW750 and SnW900 are Sn-functionalised wood biomass (W)-based catalysts annealed at 750 and 900 °C, respectively.

4. Conclusions

We proposed an effective and green approach for upcycling wood waste into Sn-functionalised biochar catalysts by solid mixing Sn source with biomass/biochar support

under solvent-free conditions in a ball mill. The SnBC catalysts were evaluated in terms of production of fructose from glucose, which is an important step in the valorisation of food waste for value-added chemical synthesis. The results indicated that different biomass/biochar supports and annealing temperatures significantly influenced the catalytic performance of SnBCs because of the variations in Sn loading rate, metal speciation, and surface chemistry. The catalysts prepared from functional group-rich biomass (SnW750 and SnW900) presented more effective glucose-to-fructose isomerisation than SnLBs and SnHBs. An intensive annealing process facilitated the formation of active Sn species, leading to higher catalytic activity. Understanding the metal-support interactions is the key to designing cost-effective biochar catalysts serving sustainable biorefineries, which is a promising option for wood waste management.

Supporting Information

Operational conditions of HPLC; differences in XRD and FTIR spectra of pristine and reused SnW750; XPS results of reused SnW750; SEM images and surface Sn content of reused SnW750; Sn content in pristine and reused catalysts.

Acknowledgement

The authors appreciate the financial support from the Hong Kong Research Grants Council (PolyU 15217818) and Hong Kong International Airport Environmental Fund (Phase 2).

References

Baca, M., de la Rochefoucauld, E., Ambroise, E., Krafft, J.M., Hajjar, R., Man, P.P., Carrier, X., Blanchard, J., 2008. Characterization of mesoporous alumina prepared by surface alumination of SBA-15, Microporous Mesoporous Mater. 110, 232–241.

Bermejo-Deval, R., Orazov, M., Gounder, R., Hwang, S.J., Davis, M.E., 2014. Active sites in Sn-Beta for glucose isomerization to fructose and epimerization to mannose. ACS Catal., 4, 2288-2297.

Cao, L., Yu, I.K.M., Chen, S.S., Tsang, D.C.W., Wang, L., Xiong, X., Zhang, S., Ok, Y.S., Kwon, E.E., Song, H., Poon, C.S., 2018. Production of 5-hydroxymethylfurfural from starch-rich food waste catalyzed by sulfonated biochar, Bioresour. Technol. 252, 76–82.

Caratzoulas, S., Davis, M.E., Gorte, R.J., Gounder, R., Vlachos, D.G., 2014. Challenges of and insights into acid-catalyzed transformations of sugars, J. Phys. Chem. C. 118, 22815–22833.

Cao, L., Yu, I.K.M., Tsang, D.C.W., Zhang, S., Ok, Y.S., Kwon, E.E., Song, H., Poon, C.S., 2018. Phosphoric acid-activated wood biochar for catalytic conversion of starch-rich food waste into glucose and 5-hydroxymethylfurfural, Bioresour. Technol. 267, 242–248.

Chen, S.S., Maneerung, T., Tsang, D.C.W., Ok, Y.S., Wang, C.H., 2017. Valorization of biomass to hydroxymethylfurfural, levulinic acid, and fatty acid methyl ester by heterogeneous catalysts, Chem. Eng. J. 328, 246–273.

Chen, S.S., Yu, I.K.M., Cho, D.W., Song, H., Tsang, D.C.W., Tessonnier, J.P., Ok, Y.S., Poon, C.S., 2018. Selective glucose isomerization to fructose via a nitrogen-doped solid base catalyst derived from spent coffee grounds, ACS Sustain. Chem. Eng. 6, 16113–16120.

Cho, D.W., Yoon, K., Ahn, Y., Sun, Y., Tsang, D.C.W., Hou, D., Ok, Y.S., Song, H., 2019. Fabrication and environmental applications of multifunctional mixed metal-biochar composites (MMBC) from red mud and lignin wastes. J. Hazard. Mater., 374, 412-419.

Farahani, S.K.V., Veal, T.D., Mudd, J.J., Scanlon, D.O., Watson, G.W., Bierwagen, O., White, M.E., Speck, J.S., McConville, C.F., 2014. Valence-band density of states and surface electron accumulation in epitaxial SnO2 films, Phys. Rev. B 90, 155413.

Dijkmans, J., Dusselier, M., Gabriëls, D., Houthoofd, K., Magusin, P.C.M.M., Huang, S., Pontikes, Y., Trekels, M., Vantomme, A., Giebeler, L., Oswald, S., Sels, B.F., 2015. Cooperative catalysis for multistep biomass conversion with Sn/Al beta zeolite, ACS Catal. 5, 928–940.

Franco, A., De, S., Balu, A.M., Garcia, A., Luque, R., 2017. Mechanochemical synthesis of graphene oxide-supported transition metal catalysts for the oxidation of isoeugenol to vanillin, Beilstein J. Org. Chem. 13, 1439–1445.

Freiser, H., 1959. Gas-liquid partition chromatography for metals separations, Anal. Chem. 31, 1440.

Hafizi, H., Najafi Chermahini, A., Saraji, M., Mohammadnezhad, G., 2016. The catalytic conversion of fructose into 5-hydroxymethylfurfural over acid-functionalized KIT-6, an ordered mesoporous silica, Chem. Eng. J. 294, 380–388.

Hassan, S.S., Williams, G.A., Jaiswal, A.K., 2019. Moving towards the second generation of lignocellulosic biorefineries in the EU: Drivers, challenges, and opportunities. Renew. Sustain. Energ. Rev., 101, 590-599.

Hu, L., Song, Y., Saravanamurugan, S., Riisager, A., 2017. Glucose isomerization by enzymes and chemo-catalysts: Status and current advances, ACS Catal. 7, 3010–3029.

Igalavithana, A.D., Park, J., Ryu, C., Lee, Y.H., Hashimoto, Y., Huang, L., Kwon, E.E., Ok, Y.S., Lee, S.S., 2017. Slow pyrolyzed biochars from crop residues for soil metal(loid) immobilization and microbial community abundance in contaminated agricultural soils, Chemosphere 177, 157–166.

Igalavithana, A.D., Yang, X., Zahra, H.R., Tack, F.M.G., Tsang, D.C.W., Kwon, E.E., Ok, Y.S., 2018. Metal(loid) immobilization in soils with biochars pyrolyzed in N2 and CO2 environments, Sci. Total Environ. 630, 1103–1114.

James, S.L., Adams, C.J., Carsten, B., Dario, B., Paul, C., Tomislav, F., Fabrizia, G., Harris, K.D.M., Geoff, H., William, J., 2011. Mechanochemistry: Opportunities for new and cleaner synthesis, Chem. Soc. Rev. 41, 413–447.

Jung, K.W., Lee, S.Y., Choi, J.W., Lee, Y.J., 2019. A facile one-pot hydrothermal synthesis of hydroxyapatite/biochar nanocomposites: Adsorption behavior and mechanisms for the removal of copper(II) from aqueous media, Chem. Eng. J. 369, 529–541.

Jung, Y., Yang, W., Koo, C.Y., Song, K., Moon, J., 2012. High performance and high stability low temperature aqueous solution-derived Li-Zr co-doped ZnO thin film transistors, J. Mater. Chem. 22, 5390–5397.

Kathryn, R., Christopher, H., James, S.L., 2013. Application of heterogeneous catalysts prepared by mechanochemical synthesis, Chem. Soc. Rev. 42, 7701–7718.

Li, Y., Zimmerman, A.R., He, F., Chen, J., Han, L., Chen, H., Hu, X., Gao, B., 2020. Solvent-free synthesis of magnetic biochar and activated carbon through ball-mill extrusion with Fe_3O_4 nanoparticles for enhancing adsorption of methylene blue. Sci. Total Environ., p.137972.

Lin, X., Liang, Y., Lu, Z., He, L., Wu, D., 2017. Mechanochemistry: A green, activation-free and top-down strategy to high-surface-area carbon materials, ACS Sustain. Chem. Eng. 5, 8535–8540.

Lobos, M.L.N., Sieben, J.M., Comignani, V., Duarte, M., Volpe, M.A., Moyano, E.L., 2016. Biochar from pyrolysis of cellulose: An alternative catalyst support for the electro-oxidation of methanol, Int. J. Hydrogen Energy. 41, 10695–10706.

Ma, H., Teng, K., Fu, Y., Song, Y., Wang, Y., Dong, X., 2011. Synthesis of visible-light responsive Sn-SnO2/C photocatalyst by simple carbothermal reduction, Energy Environ. Sci. 4, 3067–3073.

Ok, Y.S., Chang, S.X., Gao, B., Chung, H.J., 2015. SMART biochar technology-A shifting paradigm towards advanced materials and healthcare research, Environ. Technol. Innov. 4 , 206–209.

Ouyang, W., Kuna, E., Yepez, A., Balu, A.M., Romero, A.A., Colmenares, J.C., Luque, R., 2016. Mechanochemical synthesis of TiO2 nanocomposites as photocatalysts for benzyl alcohol photo-oxidation, Nanomaterials 6, 93.

Pino, L., Vita, A., Laganà, M., Recupero, V., 2014. Hydrogen from biogas : Catalytic tri-reforming process with Ni/LaCeO mixed oxides, Appl. Catal. B-Environ. 148–149, 91–105.

Qiang, F., Wagner, T., 2007. Interaction of nanostructured metal overlayers with oxide surfaces, Surf. Sci. Rep. 62, 431–498.

Qin, C., Wang, H., Yuan, X., Xiong, T., Zhang, J., Zhang, J., 2019. Understanding structure–performance correlation of biochar materials in environmental remediation and electrochemical devices, Chem. Eng. J. 122977.

Rightmire, N.R., Hanusa, T.P., 2016. Advances in organometallic synthesis with mechanochemical methods, Dalt. Trans. 45, 2352–2362.

Ruan, X., Sun, Y., Du, W., Tang, Y., Liu, Q., Zhang, Z., Doherty, W., Frost, R.L., Qian, G., Tsang, D.C.W., 2019. Formation, characteristics, and applications of environmentally persistent free radicals in biochars: a review. Bioresour. Technol., 281, 457-468.

Sikarwar, V.S., Zhao, M., Clough, P., Yao, J., Zhong, X., Memon, M.Z., Shah, N., Anthony, E., Fennell, P., 2016. An overview of advances in biomass gasification, Energy Environ. Sci. 9, 2927–3304.

Sun, Y., Yu, I.K.M., Tsang, D.C.W., Cao, X., Lin, D., Wang, L., Graham, N.J., Alessi, D.S., Komárek, M., Ok, Y.S., Feng, Y., 2019. Multifunctional iron-biochar composites for the removal of potentially toxic elements, inherent cations, and hetero-chloride from hydraulic fracturing wastewater. Environ. Int., 124, 521-532.

Takacs, L., 2018. Two important periods in the history of mechanochemistry, J. Mater. Sci., 1–7.

Wan, Z., Sun, Y., Tsang, D.C.W., Yu, I.K.M., Fan, J., Clark, J.H., Zhou, Y., Cao, X., Gao, B., Ok, Y.S., 2019. A sustainable biochar catalyst synergized with copper heteroatoms and CO_2 for singlet oxygenation and electron transfer routes. Green Chem., 21, 4800-4814.

Wang, L., Chen, L., Tsang, D.C.W., Kua, H.W., Yang, J., Ok, Y.S., Ding, S., Hou, D., Poon, C.S., 2019. The roles of biochar as green admixture for sediment-based construction products. Cem. Concr. Compos., 104, 103348.

Xiao, L.P., Wang, S., Li, H., Li, Z., Shi, Z.J., Xiao, L., Sun, R.C., Fang, Y., Song, G., 2017. Catalytic hydrogenolysis of lignins into phenolic compounds over carbon nanotube supported molybdenum oxide, ACS Catal. 7, 7535–7542.

Xiong, X., Yu, I.K.M., Cao, L., Tsang, D.C.W., Zhang, S., Ok, Y.S., 2017. A review of biochar-based catalysts for chemical synthesis, biofuel production, and pollution control, Bioresour. Technol. 246, 254–270.

524 Xiong, X., Yu, I.K.M., Tsang, D.C.W., Bolan, N.S., Ok,Y.S., Igalavithana, A.D.,
525 Kirkham, M.B., Kim, K.H., Vikrant,K., 2019. Value-added chemicals from food supply
526 chain wastes: State-of-the-art review and future prospects, Chem. Eng. J. 375, 121983.

527 Yang, X., Jin, D., Zhang, M., Wu, P., Jin, H., Li, J., Wang, X., Ge, H., Wang, Z., Lou, H.,
528 2016. Fabrication and application of magnetic starch-based activated hierarchical porous
529 carbon spheres for the ef fi cient removal of dyes from water, Mater. Chem. Phys. 174,
530 179–186.

531 Yang, X., Kwon, E.E., Dou, X., Zhang, M., Kim, K., Tsang, D.C.W., Ok, Y.S., 2018.
532 Frbrication of spherical biochar by a two-step thermal process from waste potato peel,
533 Sci. Total Environ. 626, 478–485.

534 Yang, X., Ng, W., Shu, B., Wong, E., Hun, G., Wang, C., 2019b. Characterization and
535 ecotoxicological investigation of biochar produced via slow pyrolysis : Effect of
536 feedstock composition and pyrolysis conditions, J. Hazard. Mater. 365, 178–185.

537 Yang, X., Yu, I.K.M., Cho, D., Chen, S.S., Tsang, D.C.W., Shang, J., Yip, A.C.K., Wang,
538 L., Ok, Y.S., 2019a. Tin-functionalized wood biochar as a sustainable solid catalyst for
539 glucose isomerization in biorefinery, ACS Sustain. Chem. Eng. 7, 4851–4860.

540 Yu, I.K.M., Xiong, X., Tsang, D.C.W., Wang, L., Hunt, A.J., Song, H., Shang, J., Ok,
541 Y.S., Poon, C.S., 2019a. Aluminium-biochar composites as sustainable heterogeneous
542 catalysts for glucose isomerisation in a biorefinery, Green Chem. 21, 1267–1281.

543 Yu, I.K.M., Xiong, X., Tsang, D.C.W., Ng, Y.H., Clark, J.H., Fan, J., Zhang, S., Hu, C.,
544 Ok, Y.S., 2019b. Graphite oxide- and graphene oxide-supported catalysts for microwave-
545 assisted glucose isomerisation in water, Green Chem. 21, 4341–4353.

546 Yu, I.K.M., Tsang, D.C.W., Yip, A.C.K., Hunt, A.J., Sherwood, J., Shang, J., Song, H.,
547 Ok, Y.S., Poon, C.S., 2018. Propylene carbonate and γ-valerolactone as green solvents
548 enhance Sn(IV)-catalysed hydroxymethylfurfural (HMF) production from bread waste,
549 Green Chem. 20, 2064–2074.

550 Yu, J., Tang, L., Pang, Y., Zeng, G., Wang, J., Deng, Y., Liu,Y., Feng, H., Chen, S., Ren,
551 X., 2019c. Magnetic nitrogen-doped sludge-derived biochar catalysts for persulfate
552 activation: Internal electron transfer mechanism, Chem. Eng. J. 364, 146–159.

553 Zatsepin, D.A., Zatsepin, A.F., Boukhvalov, D.W., Kurmaev, E.Z., Gavrilov, N. V., 2016.
554 Sn-loss effect in a Sn-implanted a-SiO2 host-matrix after thermal annealing: A combined
555 XPS, PL, and DFT study, Appl. Surf. Sci. 367, 320–326.

556 Zhang, Q., Wang, J., Lyu, H., Zhao, Q., Jiang, L., Liu, L., 2019. Ball-milled biochar for
557 galaxolide removal: Sorption performance and governing mechanisms, Sci. Total
558 Environ. 659, 1537–1545.

559 Zhu, Y., Romain, C., Williams, C.K., 2016a. Sustainable polymers from renewable
560 resources, Nature 540, 354–362.

561 Zhu, H., Rosenfeld, D.C., Harb, M., Anjum, D.H., Hedhili, M.N., Ould-Chikh, S., Basset,
562 J.M., 2016b. Ni-M-O (M = Sn, Ti, W) catalysts prepared by a dry mixing method for
563 oxidative dehydrogenation of ethane, ACS Catal. 6, 2852–2866.

564 Zhukovskii, Y.F., Kotomin, E.A., Jacobs, P.W., Stoneham, A.M., 2000. Ab initio
565 modeling of metal adhesion on oxide surfaces with defects, Phys. Rev. Lett. 84, 1256.

566 Zhong, J., Xia, Z., Luo, M., Zhao, J., Chen, J., Wang, L., Liu, X., Xue, D.J., Cheng, Y.B.,
567 Song, H., Tang, J., 2014. Sulfurization induced surface constitution and its correlation to
568 the performance of solution-processed $Cu_2ZnSn(S,Se)_4$ solar cells, Sci. Rep. 4, 6288.

569

570 For Table of Contents Use Only

571 The Sn-functionalised catalyst synthesised by ball milling shows effective catalytic activity

572 for glucose isomerisation.

573

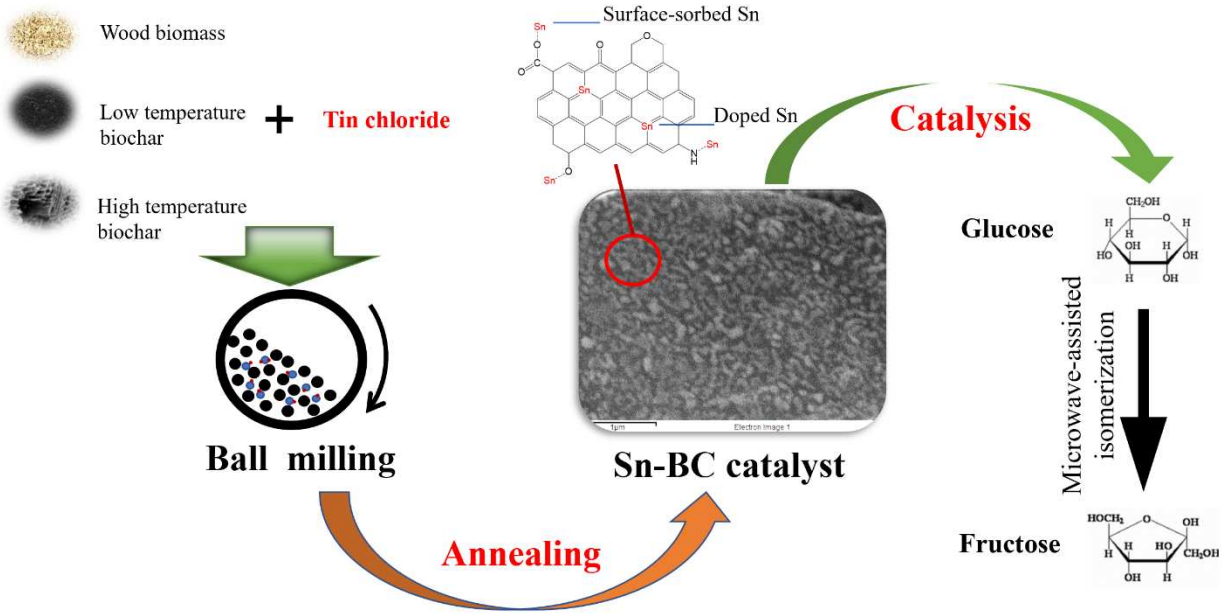

574

575

576

Highlights:

- Sn-functionalized biochar catalysts were synthesized via solvent-free ball milling.
- The sustainable biochar catalysts promoted glucose-to-fructose isomerization.
- Supporting materials and annealing temperatures determined catalytic activity.
- Metal-support interactions governed Sn loading and its speciation.

Declaration of interests

☒ The authors declare that they have no known competing financial interests or personal relationships that could have appeared to influence the work reported in this paper.

☐The authors declare the following financial interests/personal relationships which may be considered as potential competing interests: